

LES-Study of Gas Bubbles and Liquid Metal Turbulent MHD-Flow for Different Parameters

S. Pavlovs, A. Jakovics, V. Sushkovs, E. Baake

Abstract

The paper presents the transient distributions of physical fields for turbulent nitrogen bubbles flow through *Wood-metal* in *rectangle bubble reactor (RBR)*, which is placed in the external uniform magnetic field. For multiphase flow *LES (Large Eddy Simulation)* study the experimentally verified (without magnetic field) *Euler-Euler* approach is used, which is realized with *ANSYS Fluent Magnetohydrodynamic (MHD) module*. The computational results are compared with corresponding results for *RBR*, when continuous phase is electrically conductive ‘water-like’ liquid and dispersed phase is air bubbles. The trends for gas jet rising speed in liquid (the transition process is considered) without and with external magnetic field are compared with corresponding trends for *cylindrical bubble reactor (CBR)*.

1. Introduction

The results, presented in current paper, are obtained with application of previously formulated computational model (see detailed description in [1]), which includes:

- continuity equation, volume conservation equation and momentum equations for turbulent two-phase *MHD-flow*, driven by gas injected into electrically conductive liquid, which is placed into external uniform magnetic field;
- equations for induction of magnetic field, induced by flow of electrically conductive liquid in external magnetic field.

The momentum equations include interfacial (buoyancy and drag) forces and external body (*Lorentz*) force.

The drag force is computed with application of several classical models, including:

- *Schiller-Naumann* model [2] as well as *Newton* or *Stokes* models for undistorted (spherical) bubbles; the choice of models is performed according to the local value of bubble *Reynolds* number (Re_g) – see [1, equation (13)];
- *Grace* model [3] for distorted (elliptical) bubbles with *Morton* and *Evötös* numbers, which characterize the shape of moving bubbles and represent the correlations between the tension at gas-liquid surface, the inertia and the viscosity of liquid.

The peculiarities of numerical computations of turbulent two-phase *MHD-flow* using *Euler-Euler* approach, realized in *ANSYS Fluent MHD module*, are discussed in [1,4].

The experimental verification of developed numerical model the available measurement data has been used for air–water *RBR* [5], air–water *CBR* [6] and nitrogen–*Wood-metal CBR* without external magnetic field [7] – the predicted and measured profiles of vertical (axial) velocity of liquid are of a good qualitative and quantitative agreement [4]. For argon–*GalSn-alloy CBR* [8], placed into external longitudinal or transversal magnetic field, our computations are still continuing; the obtained up to now velocity profiles show a good qualitative agreement with measurement [8] and computation [9] results.

2. Geometry and operational parameters of bubble reactors

The geometry and operational parameters of considered nitrogen–*Wood*-metal *RBR* are gathered in Tab. 1. This *RBR* geometry corresponds to air–water experimental setup [5]. For the further comparison of computational results, the nitrogen–*Wood*-metal *CBR* [1] is used with geometry, which corresponds to experimental setup [7].

Note, that due to large inlet opening the mass flow rate for *RBR* is relatively large.

Tab. 1. Bubble reactors' geometry* and operational parameters

Geo- metry	Gas-liquid two-phase system	Reactor, $L \times W$ or D (m)	Liquid +gas, H (m)	Inlet opening, $L \times W$ or D (mm)	Gas bubble diameter (mm)	Gas volume flow (cm^3/s)	Gas mass flow (g/s)	Gas velocity at inlet (m/s)
<i>RBR</i>	N_2 - <i>Wood</i> -metal	0.5×0.2	1.5+0.5	180×80	0.5	6800	8.500	0.47
<i>RBR</i>	Air-‘water-like’ liquid**				3			
<i>CBR</i>	N_2 - <i>Wood</i> -metal	0.4	0.4+0.2	10	3 or 0.1	200	0.250	2.58

* height (H); length (L) and width (W) for *RBR*; diameter (D) for *CBR*

** for “water-like” liquid the electrical conductivity is assigned (see Tab. 2)

During previous computations for air–water *RBR* [4] in order to consider the two-phase *MHD*-flows in external magnetic field, the electrical conductivity has been assigned for liquid, which further is called the electrical conductive ‘water-like’ liquid. The physical parameters for two-phase systems – nitrogen–*Wood*-metal and air-‘water-like’ liquid – are gathered in Tab. 2.

Note, that *Wood*-metal density is greater than ‘water-like’ liquid density for an order.

For reference: density of liquid sodium near melting point is $0.927 \cdot 10^3 \text{ kg/m}^3$ (close to water density); electrical conductivity of liquid sodium is varying from $10 \cdot 10^6 \text{ } \Omega^{-1} \cdot m^{-1}$ till $1.2 \cdot 10^6 \text{ } \Omega^{-1} \cdot m^{-1}$ for temperature range from melting point ($97.8^\circ C$) till boiling point ($882.4^\circ C$).

Tab. 2. Physical parameters of gas-liquid two-phase systems

Physical parameter	Nitrogen (N_2)	<i>Wood</i> -metal	Air	‘Water- like’ liquid
Operation temperature ($^\circ C$)	75		room	
State	ideal gas	liquid metal	ideal gas	liquid
Molar mass ($kg/kmol$)	28.01	–	28.96	–
Density (kg/m^3)	1.251	$9.65 \cdot 10^3$	1.204	$0.997 \cdot 10^3$
Thermal expansion coefficient (K^{-1})	–	$25 \cdot 10^{-4}$	–	$2.57 \cdot 10^{-4}$
Dynamic viscosity ($kg/(m \cdot s)$)	$1.77 \cdot 10^{-5}$	$3.26 \cdot 10^{-3}$	$1.83 \cdot 10^{-5}$	$0.89 \cdot 10^{-3}$
Gas–liquid surface tension coefficient (N/m^{-1})	0.42		0.072	
Electrical conductivity ($\Omega^{-1} \cdot m^{-1}$)	–	$2.5 \cdot 10^6$	–	10^6

The qualitative estimation of relationship between *Lorentz* and inertia forces as well as *Lorentz* and viscous forces for *MHD*-flow of liquid phase can be made with *Stuart* and *Hartmann* number accordingly – see [1, equations (29) and (30)]. For considered *RBR* as well as for *RBR* and *CBR*, which are used for comparison, the estimations are gathered in Tab. 3.

According to estimations for all considered reactors – *Stuart* number is $N < 1$ and *Hartmann* number is $Ha \gg 1$ – thus the structure of resultant *MHD*-flow of conductive liquid in *RBR* more preferably depends on prevailing of inertia forces in the liquid in the case of relatively large value of inlet gas flow rate, where the characteristic size of intensive flow is substantially smaller than size of container horizontal cross-section and can be measured with characteristic size of horizontal cross-section of bubble jet.

Tab. 3. Non-dimensional numbers for bubble reactors

Geo- metry	Gas-liquid two-phase system	Liquid maximum velocity (<i>m/s</i>)	Bubble <i>Reynolds</i> number Re_g	Induction of external magnetic field (<i>T</i>)	<i>Stuart</i> number <i>N</i>	<i>Hartmann</i> Number <i>Ha</i>
<i>RBR</i>	N_2 – <i>Wood</i> -metal	~2	~580	0.1	~0.65	~1385
<i>RBR</i>	Air–‘water-like’ liquid	~2.9	~320	0.1	~0.7	~670
<i>CBR</i>	N_2 – <i>Wood</i> -metal	~1.6	~335	0.1	~0.35	~550

It is necessary also to take into account the following features of closed flow:

- the liquid velocity, averaged for horizontal cross-section of container, is zero;
- the reverse flow is closed in peripheral zone of liquid container.

3. Computational results

The computational results for *RBR* (Tabs. 1–3) are presented in Figs. 1–3.

The visualization of physical fields is performed with *ANSYS CFD Post* and there are definite compromises:

√ To gain visualization of liquid flow patterns in the whole volume, but not only near gas jet, the liquid streamlines are presented with inverse grey scale (Fig. 3). Thus black streamlines present the flow with small velocity values. In the gas layer, which is located above liquid, where the values of liquid volume fraction are close to zero, the black streamlines for liquid are visualized as well. The streamlines, which correspond to large velocity values, are white and thus are invisible (Fig. 3).

√ If for visualization would be chosen grey scale, the black streamlines would present only the liquid flow with large velocity values – the distribution of such streamlines would be similar to distribution of gas volume fraction in gas jet (Fig. 2). In this case the liquid flow streamlines in the rest of liquid volume would be white and thus would be invisible.

3.1. Liquid density and *MHD*-flow structure

The computations for relatively light ($\rho_l = 0.997 \cdot 10^3 \text{ kg/m}^3$) electrically conductive ‘water-like’ liquid in *RBR* (Tabs. 1–3) show, that the magnetic field is stabilizing the liquid *MHD*-flow in reactor, makes it less chaotic and consequently is regularizing gas flow – compare Fig. 1 (a,b) and Fig. 1 (c,d).

The computations for relatively heavy ($\rho_l = 9.650 \cdot 10^3 \text{ kg/m}^3$) *Wood*-metal in *RBR* (Tabs. 1–3) show, that the application of magnetic field in reactor does not homogenize the gas distribution in volume of liquid metal. On contrary, the high-speed gas jet remain after switching on magnetic field – compare Fig. 2 (a,b) and Fig 2 (c,d).

3.2. Influence of bubbles size on gas jet penetration into liquid

For the case of relatively large bubbles ($d_g=3\cdot 10^{-3}$ m) the air jet in *RBR* (Tabs. 1–3) rises faster in electrically conductive water-like liquid, when external magnetic field is switched on if compare with the case without magnetic field.

The inverse trend is found for the case of relatively small bubbles ($d_g=0.5\cdot 10^{-3}$ m). The nitrogen bubbles in *RBR* (Tabs. 1–3) rises faster in *Wood*-metal without magnetic field if compare with the case when magnetic field is switched on.

Similar trends are found in computational results for nitrogen–*Wood*-metal *CBR* (Tabs. 1–3), obtained in [1] for relatively large ($d_g=3\cdot 10^{-3}$ m) and relatively small ($d_g=0.1\cdot 10^{-3}$ m) bubbles – see [1, Fig. 5].

These effects can be explained by competition of two phenomena:

- the damping effect of *Lorentz* force [10], which acts to turbulent vortices, and therefore makes smaller the turbulent resistance for gas bubble flow;
- the increasing (or decreasing) of total resistance for bubble flow for smaller (or larger) diameter of bubbles due to increasing (or decreasing) of total surface of bubbles in volume unit and therefore increasing (or decreasing) of drag force.

The competition of mentioned phenomena, when magnetic field is switched on, results in acceleration of considered *MHD*-flow [4, Fig. 3] for relatively large bubbles ($d_g=3\cdot 10^{-3}$ m); but in the case of relatively small bubbles ($d_g=0.5\cdot 10^{-3}$ m) the result is opposite – *MHD*-flow is decelerated (Fig. 3).

As the confirmation of this effect the experimental results for rising single bubble [11] can be considered (note, that interval of parameters for single bubble and considered collective bubble dynamics are different) – the drag coefficient for larger bubble is decreasing, when magnetic field is switched on; for smaller bubbles the effect of magnetic field is opposite – the drag coefficient is increasing.

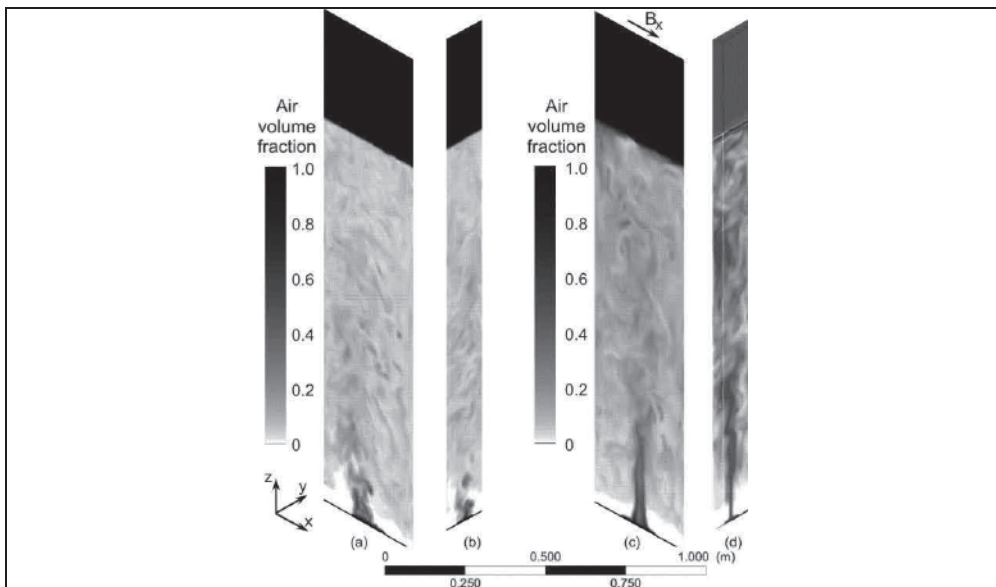


Fig. 1. Air-‘water-like’ liquid *RBR* – cross-sections: (a, c) $y=0$ and (b, d) $x=0$.

Instantaneous (flow time $t = 20$ s) contours of air volume fraction:

(a, b) without magnetic field $B = 0$; (c, d) with transversal external magnetic field $B_x = 0.1$ T

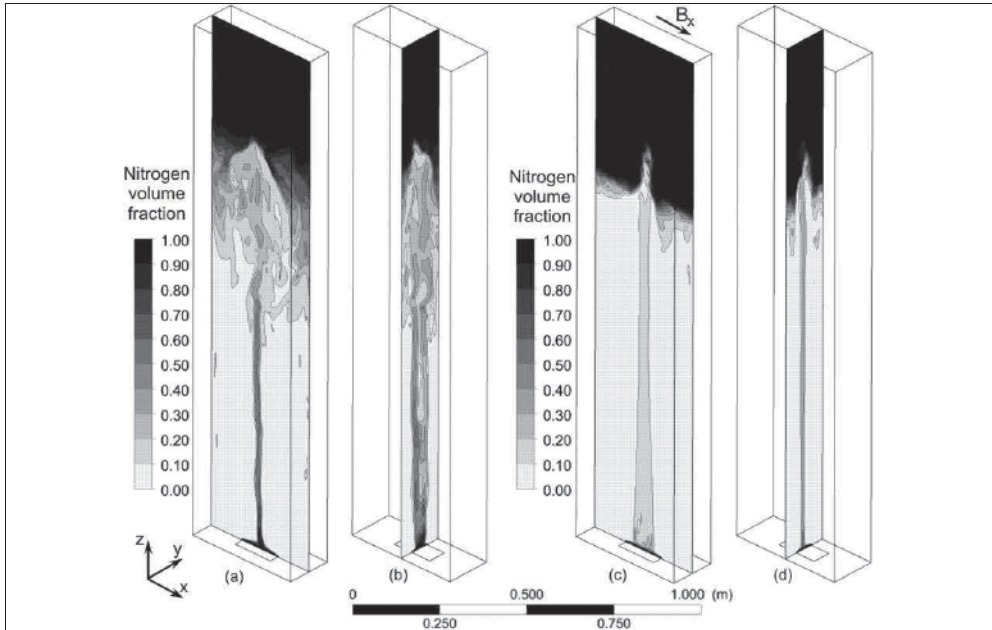


Fig. 2. N_2 -Wood-metal RBR – cross-sections: (a, c) $y=0$ and (b, d) $x=0$. Instantaneous (flow time $t = 5$ s) contours of nitrogen volume fraction: (a, b) without magnetic field $B = 0$; (c, d) with transversal external magnetic field $B_x = 0.1$ T

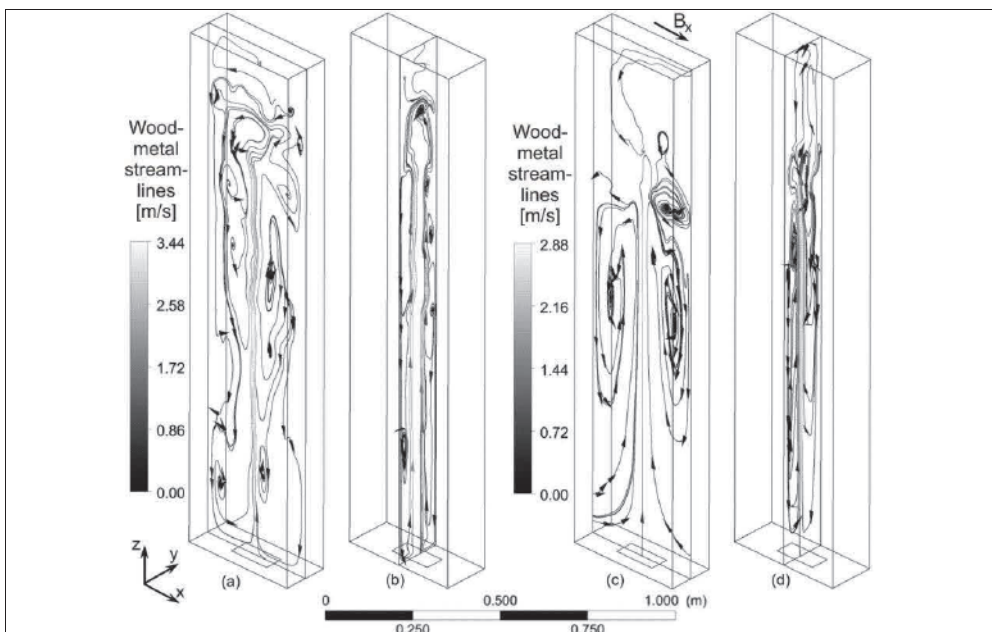


Fig. 3. N_2 -Wood-metal RBR – cross-sections: (a, c) $y=0$ and (b, d) $x=0$. Instantaneous (flow time $t = 5$ s) Wood-metal streamlines in peripheral zone of container: (a, b) without magnetic field $B = 0$; (c, d) with transversal external magnetic field $B_x = 0.1$ T

4. Conclusions and outlook

For flow of bubbles with larger and smaller diameters, there are different trends for gas rising speed in liquid metal without and with external magnetic field: the larger bubbles rise faster in liquid, when magnetic field is switched on, but the smaller bubbles – in opposite, when magnetic field is switched off.

To obtain the wider information on mentioned trends the in-depth analysis of reactors' parameters is planned.

The aim of further computations is the case, when $N \gg 1$ and $Ha \gg 1$ – that is Lorentz force is prevailing both in the zone of gas jet and in the zone near the wall.

Acknowledgment

The current research is supported by the *Helmholtz Association of German Research Centers*, within the scope of the *Helmholtz Alliance – Liquid Metal Technologies (LIMTECH)*.

References

- [1] Pavlovs, S., Jakovics, A., Sushkovs, V., Baake, E.: *Gas bubbles and electrically conductive liquid turbulent flow in uniform magnetic field*. Magnetohydrodynamics, Vol. 53, 2017 (in press).
- [2] Schiller, L., Naumann, A.Z.: *Über die grundlegenden Berechnungen bei der Schwerkraftaufbereitung*. Zeitschrift des Vereins Deutscher Ingenieure für Maschinenbau und Metallbearbeitung (VDI-Z), Bd. 77, 1933, S. 318–320.
- [3] Clift, R., Grace, J.R., Weber, M.E.: *Bubbles, drops and particles*. Academic Press, New Your, 1978, 380 p.
- [4] Pavlovs, S., Jakovics, A., Sushkovs, V., Baake, E.: *Influence of magnetic field on gas bubbles flow in liquid metal*. International Journal of Applied Electromagnetics and Mechanics (IJAE), 2017, Vol. 53, No. S1, pp. S31–S41.
- [5] Sanchez-Forero, D.I., Silva (Jr.), J.L., Silva, M.K., Bastos, J.C.S.C., Mori, M.: *Experimental and numerical investigation of gas-liquid flow in a rectangular bubble column with centralized aeration flow pattern*. Chemical Engineering Transactions, Vol. 32, 2013, pp. 1561–1566.
- [6] Lou, W., Zhu, M.: *Numerical simulation of gas and liquid two-phase flow in gas-stirred systems based on Euler–Euler approach*. Metallurgical and Materials Transactions B, Vol. 44, 2013, pp. 2013–2021.
- [7] Xie, Y., Oeters, F.: *Experimental studies on the flow velocity of molten metals in a ladle model at centric gas blowing*. Steel Research International, Vol. 63, 1992, No. 3, pp. 93–104.
- [8] Zhang, C., Eckert, S., Gerbeth, G.: *Modification of bubble-driven liquid metal flows under the influence of a DC magnetic field*. ISIJ International, Vol. 47, 2007, No. 6, pp. 795–801.
- [9] Miao, X., Lucas, D., Ren, Z., Eckert, S., Gerbeth, G.: *Numerical modeling of bubble-driven liquid metal flows with external static magnetic field*. International Journal of Multiphase Flow, Vol. 48, 2013, pp. 32–45.
- [10] Gelfgat, Yu.M., Lielausis, O.A., Shcherbinin, E.V.: *Liquid metal under the influence of electromagnetic forces*. Science, Riga (Latvia), 1976, 248 p. (in Russian).
- [11] Xie, Y.: *Untersuchung der Strömung und des Blasenverhaltens in gasgerührten Wood-Metall-Schmelzen*. Doktor-Ingenieur Dissertation. Technischen Universität, Berlin (German), 1991, 249 p.

Authors

Dr.-Phys. Pavlovs, Sergejs
 Prof. Dr.-Phys. Jakovics, Andris
 B.Sc.-Phys. Sushkovs, Vadims
 Laboratory for Mathematical Modelling
 of Environmental and Technological Processes
 University of Latvia
 Zellu str. 23, LV-1002 Riga, Latvia
 E-mail: sergejs.pavlovs@lu.lv
 E-mail: andris.jakovics@lu.lv
 E-mail: vadim.sushkov13@gmail.com

Prof. Dr.-Ing. Baake, Egbert
 Institute of Electrotechnology
 Leibniz University of Hannover
 Wilhelm-Busch-Str. 4
 D-30167 Hannover, Germany
 E-mail: baake@etp.uni-hannover.de